

Strong Enhancement of Rashba spin-orbit coupling with increasing anisotropy in the Fock-Darwin states of a quantum dot

Siranush Avetisyan,¹ Pekka Pietiläinen,² and Tapash Chakraborty^{†1}

¹*Department of Physics and Astronomy, University of Manitoba, Winnipeg, Canada R3T 2N2*

²*Department of Physics/Theoretical Physics, University of Oulu, Oulu FIN-90014, Finland*

We have investigated the electronic properties of elliptical quantum dots in a perpendicular external magnetic field, and in the presence of the Rashba spin-orbit interaction. Our work indicates that the Fock-Darwin spectra display strong signature of Rashba spin-orbit coupling even for a low magnetic field, as the anisotropy of the quantum dot is increased. An explanation of this pronounced effect with respect to the anisotropy is presented. The strong spin-orbit coupling effect manifests itself prominently in the corresponding dipole-allowed optical transitions, and hence is susceptible to direct experimental observation.

In recent years our interest in understanding the unique effects of the spin-orbit interaction (SOI) in semiconductor nanostructures [2] has peaked, largely due to the prospect of the possible realization of coherent spin manipulation in spintronic devices [3], where the SOI is destined to play a crucial role [4]. As the SOI couples the orbital motion of the charge carriers with their spin state, an all-electrical control of spin states in nanoscale semiconductor devices could thus be a reality. In this context the Rashba SOI [5] has received particular attention, largely because in a two-dimensional electron gas the strength of the Rashba SOI has already been shown to be tuned by the application of an electric field [6]. While the earlier studies were primarily in a two-dimensional electron gas, the attention has now been focused on the role of SOI in a single InAs quantum dot [7]. The quantum dot (QD) [8], a system of few electrons confined in the nanometer region has the main advantage that the shape and size of the confinement can be externally controlled, which provides an unique opportunity to study the atomic-like properties of these systems [8, 9]. SO coupling in quantum dots generates anisotropic spin splitting [10] which provides important information about the SO coupling strength.

Extensive theoretical studies of the influence of Rashba SOI in circularly symmetric parabolic confinement have already been reported earlier [11], where the SO coupling was found to manifest itself mainly in multiple level crossings and level repulsions. They were attributed to an interplay between the Zeeman and the SOI present in the system Hamiltonian. Those effects, in particular, the level repulsions were however weak and as a result, would require extraordinary efforts to detect the strength of SO coupling [12] in those systems. Here we show that, by introducing anisotropy in the QD, i.e., by breaking the circular symmetry of the dot, we can generate a major enhancement of the Rashba SO coupling effects in a quantum dot. As shown below, this can be observed directly in the Fock-Darwin states of a QD, and therefore should be experimentally observable [8, 9]. We show below that the Rashba SO coupling effects are manifestly

strong in an elliptical QD [13], which should provide a direct route to unambiguously determine (and control) the SO coupling strength. It has been proposed recently that the anisotropy of a quantum dot can also be tuned by an in-plane magnetic field [14].

The Fock-Darwin energy levels in elliptical QDs subjected to a magnetic field was first reported almost two decades ago [13], where it was found that the major effect of anisotropy was to lift the degeneracies of the single-particle spectrum [15]. The starting point of our present study is the stationary Hamiltonian

$$\begin{aligned}\mathcal{H}_S &= \frac{1}{2m^*} \left(\mathbf{p} - \frac{e}{c} \mathbf{A}_S \right)^2 + V_{\text{conf}}(x, y) + \mathcal{H}_{\text{SO}} + \mathcal{H}_z \\ &= \mathcal{H}_0 + \mathcal{H}_{\text{SO}} + \mathcal{H}_z\end{aligned}$$

where the confinement potential is chosen to be of the form

$$V_{\text{conf}} = \frac{1}{2} m^* (\omega_x^2 x^2 + \omega_y^2 y^2),$$

$\mathcal{H}_{\text{SO}} = \frac{\alpha}{\hbar} [\boldsymbol{\sigma} \times (\mathbf{p} - \frac{e}{c} \mathbf{A}_S)]_z$ is the Rashba SOI, and \mathcal{H}_z is the Zeeman contribution. Here m^* is the effective mass of the electron, $\boldsymbol{\sigma}$ are the Pauli matrices, and we choose the symmetric gauge vector potential $\mathbf{A}_S = \frac{1}{2} (-y, x, 0)$. As in Ref. [13], we introduce the rotated coordinates and momenta

$$\begin{aligned}x &= q_1 \cos \chi - \chi_2 p_2 \sin \chi, \\ y &= q_2 \cos \chi - \chi_2 p_1 \sin \chi, \\ p_x &= p_1 \cos \chi + \chi_1 q_2 \sin \chi, \\ p_y &= p_2 \cos \chi + \chi_1 q_1 \sin \chi,\end{aligned}$$

where

$$\begin{aligned}\chi_1 &= -\left[\frac{1}{2}(\Omega_1^2 + \Omega_2^2)\right]^{\frac{1}{2}}, \quad \chi_2 = \chi_1^{-1}, \\ \tan 2\chi &= m^* \omega_c [2(\Omega_1^2 + \Omega_2^2)]^{\frac{1}{2}} / (\Omega_1^2 - \Omega_2^2), \\ \Omega_{1,2}^2 &= m^{*2} (\omega_{x,y}^2 + \frac{1}{4} \omega_c^2), \quad \omega_c = eB/m^* c.\end{aligned}$$

In terms of the rotated operators introduced above, the Hamiltonian \mathcal{H}_0 is diagonal [13]

$$\mathcal{H}_0 = \frac{1}{2m^*} \sum_{\nu=1,2} [\beta_\nu^2 p_\nu^2 + \gamma_\nu^2 q_\nu^2],$$

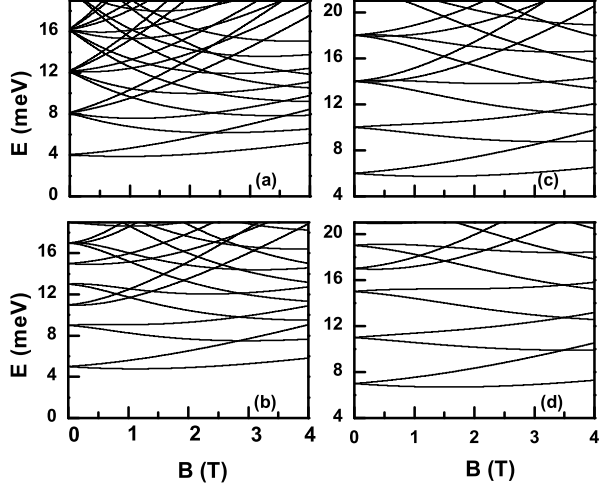


FIG. 1: Magnetic field dependence of the low-lying Fock-Darwin energy levels of an elliptical dot without the Rashba SO interaction ($\alpha = 0$). The results are for (a) $\omega_x = 4$ meV and $\omega_y = 4.1$ meV, (b) $\omega_x = 4$ meV and $\omega_y = 6$ meV, (c) $\omega_x = 4$ meV and $\omega_y = 8$ meV, and (d) $\omega_x = 4$ meV and $\omega_y = 10$ meV.

where

$$\begin{aligned}\beta_1^2 &= \frac{\Omega_1^2 + 3\Omega_2^2 + \Omega_3^2}{2(\Omega_1^2 + \Omega_2^2)}, & \gamma_1^2 &= \frac{1}{4}(3\Omega_1^2 + \Omega_2^2 + \Omega_3^2), \\ \beta_2^2 &= \frac{3\Omega_1^2 + \Omega_2^2 - \Omega_3^2}{2(\Omega_1^2 + \Omega_2^2)}, & \gamma_2^2 &= \frac{1}{4}(\Omega_1^2 + 3\Omega_2^2 - \Omega_3^2), \\ \Omega_3^2 &= \left[(\Omega_1^2 - \Omega_2^2)^2 + 2m^* \omega_c^2 (\Omega_1^2 + \Omega_2^2) \right]^{\frac{1}{2}}.\end{aligned}$$

Since the operator \mathcal{H}_0 is obviously equivalent to the Hamiltonian of two independent harmonic oscillators, the states of the electron can be described by the state vectors $|n_1, n_2; s_z\rangle$. Here the oscillator quantum numbers $n_i = 0, 1, 2, \dots$ correspond to the orbital motion and $s_z = \pm \frac{1}{2}$ to the spin orientation of the electron.

The Rashba Hamiltonian, in terms of the rotated operators is now written as,

$$\begin{aligned}\frac{\hbar}{\alpha} \mathcal{H}_{\text{SO}} &= \sigma_x (\sin \chi \chi_1 - \cos \chi \omega_0) q_1 \\ &- \sigma_y (\sin \chi \chi_1 + \cos \chi \omega_0) q_2 \\ &- \sigma_y (\cos \chi - \sin \chi \omega_0 \chi_2) p_1 \\ &+ \sigma_x (\cos \chi + \sin \chi \omega_0 \chi_2) p_2,\end{aligned}$$

where $\omega_0 = eB/2c$. The effect of the SO coupling is readily handled by resorting to the standard ladder operator formalism of harmonic oscillators and by diagonalizing \mathcal{H}_{SO} in the complete basis formed by the vectors $|n_1, n_2; s_z\rangle$.

The Fock-Darwin states in the absence of the Rashba SOI ($\alpha = 0$) are shown in Fig. 1, for $\omega_x = 4$ meV and

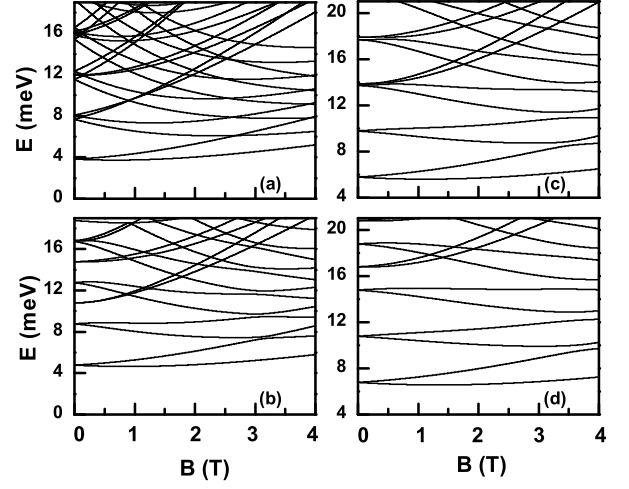


FIG. 2: Same as in Fig. 1, but for $\alpha = 20$.

$\omega_y = 4.1, 6, 8, 10$ meV in (a)-(d) respectively. We have considered the parameters of an InAs QD [11] throughout, because in such a narrow-gap semiconductor system, the dominant source of the SO interaction is the structural inversion asymmetry [16], which leads to the Rashba SO interaction. As expected, breaking of circular symmetry in the dot results in lifting of degeneracies at $B = 0$, that is otherwise present in a circular dot [13, 15]. In Fig. 1 (a), the QD is very close to being circularly symmetric, and as a consequence, the splittings of the zero-field levels are vanishingly small. As the anisotropy of the QD is increased [(b) – (d)], splitting of the levels becomes more appreciable.

As the SO term is linear in the position and momentum operators it is also linear in the raising and lowering ladder operators. It is also off-diagonal in the quantum number s_z . As a consequence, the SOI can mix only states which differ in the spin orientation, and differ by 1 either in the quantum number n_1 or in n_2 but not in both. In the case of rotationally symmetric confinements these selection rules translate to the conservation of the total angular momentum $j = m + s_z$ in the planar motion of the electron.

At the field $B = 0$ the ground states $|0, 0; \pm \frac{1}{2}\rangle$ are two-fold degenerate. Due to the selection rules, this degeneracy cannot be lifted either by the eccentricity of the dot or by the Rashba coupling. Many of the excited states, such as $|n_1, n_2; \pm \frac{1}{2}\rangle$ retain their degeneracy no matter how strong the SO coupling is or how eccentric the dot is, as we can see in the Figs. 1-3. At the same time, many other degeneracies are removed by squeezing or stretching the dot. At non-zero magnetic fields some of the crossings of the energy spectra are turned to anti-crossings by the Rashba term in the Hamiltonian. For example, the

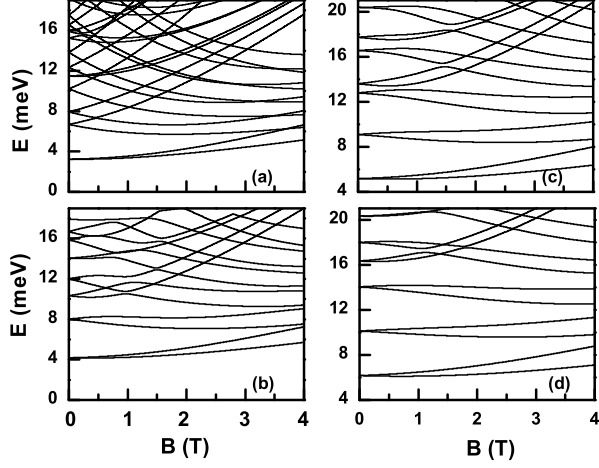


FIG. 3: Same as in Fig. 1, but for $\alpha = 40$.

second and third excited states in Fig. 2 (a) – Fig. 2 (d) are composed mainly of the states $|0, 0; \frac{1}{2}\rangle$ and $|1, 0; -\frac{1}{2}\rangle$ which are mixed by the \mathcal{H}_{SO} around $B = 3$ T causing a level repulsion. We can also see that the squeezing of the dot enhances the SO coupling. This can be thought of as a consequence of pushing some states out of the way, just as in our example of the state $|1, 1; \frac{1}{2}\rangle$. SOI mixes it with the state $|1, 0; -\frac{1}{2}\rangle$ causing the latter state to shift downward in energy thereby reducing the anti-crossing gap. Squeezing the dot, however moves the state energetically farther away from $|1, 0; -\frac{1}{2}\rangle$ and so weakens this gap reduction effect. It is abundantly clear from the features revealed in the energy spectra that for a combination of strong anisotropy of the dot and higher values of the SO coupling strength, large anti-crossing gaps would appear even for relatively low magnetic fields.

The effects of anisotropy and spin-orbit interaction on the energy spectra above are also reflected in the optical absorption spectra. Let us turn our attention on the absorption spectra for transitions from the ground state to the excited states. For that purpose we subject the dot to the radiation field

$$\mathbf{A}_R = A_0 \hat{\epsilon} \left(e^{i(\omega/c)\hat{\mathbf{n}} \cdot \mathbf{r} - i\omega t} + e^{-i(\omega/c)\hat{\mathbf{n}} \cdot \mathbf{r} + i\omega t} \right),$$

where $\hat{\epsilon}$, ω and $\hat{\mathbf{n}}$ are the polarization, frequency and the direction of propagation of the incident light, respectively. We let the radiation enter the dot along the direction perpendicular to the motion of the electron, that is parallel to the z -axis. Due to the transversality condition the polarization vector will then lie in the xy -plane.

As usual, we shall make two approximations. First we assume the intensity of the field be so weak that only the terms linear in \mathbf{A}_R has to be taken into account. Then the effect of the radiative magnetic field on the spin can

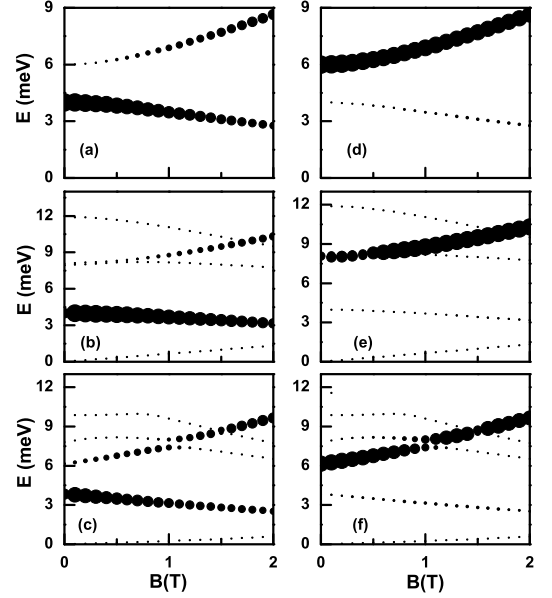


FIG. 4: Optical absorption (dipole allowed) spectra of elliptical QDs for various choice of parameters: (a) $i\alpha = 0$, $\omega_x = 4$ meV, $\omega_y = 6$, (b) $\alpha = 20$, $\omega_x = 4$ meV, $\omega_y = 8$ meV, and (c) $\alpha = 40$, $\omega_x = 4$, $\omega_y = 6$. The polarization of the incident radiation is along the x -axis. The parameters for (d)-(f) are the same, except that the incident radiation is polarized along the y -axis. The areas of the filled circles are proportional to the calculated absorption cross-section.

be neglected as well. So we can simply replace in the stationary Hamiltonian \mathcal{H}_S the vector potential \mathbf{A}_S with the field $\mathbf{A} = \mathbf{A}_S + \mathbf{A}_R$. Discarding terms higher than linear order in \mathbf{A}_R leads to the total Hamiltonian

$$\mathcal{H} = \mathcal{H}_S + \mathcal{H}_R,$$

where the radiative part \mathcal{H}_R is given by

$$\mathcal{H}_R = -\frac{e}{m_e c} \mathbf{A}_R \cdot \left(\mathbf{p} - \frac{e}{c} \mathbf{A}_S \right) - \frac{\alpha e}{\hbar c} [\boldsymbol{\sigma} \times \mathbf{A}_R]_z.$$

The radiative Hamiltonian, even in the presence of the Rashba SO coupling can be expressed in the well-known form

$$\mathcal{H}_R = i \frac{e}{\hbar c} \mathbf{A}_R \cdot [\mathbf{x}, \mathcal{H}_S],$$

\mathbf{x} being the position operator in the xy -plane.

Our second approximation is the familiar dipole approximation. We assume that the amplitude of radiation can be taken as constant within the quantum dot, so that we are allowed to write the field as

$$\mathbf{A}_R \approx A_0 \hat{\epsilon} (e^{-i\omega t} + e^{i\omega t}).$$

Since the transition energies expressed in terms of radiation frequencies are of the order of THz, the corresponding wavelengths are much larger than the typical size of a dot, thus justifying our approximation. Applying now the Fermi Golden Rule leads to the dipole approximation form

$$\sigma_{\text{abs}}(\omega) = 4\pi^2 \alpha_f \omega_{ni} |\langle n | \hat{\mathbf{e}} \cdot \mathbf{x} | i \rangle|^2 \delta(\omega_{ni} - \omega)$$

of the absorption cross section for transitions from the initial state $|i\rangle$ to the final state $|n\rangle$. Here α_f is the fine structure constant and ω_{ni} is the frequency corresponding to the transition energy $\hbar\omega$.

The familiar dipole selection rules for oscillator states dictate largely the features seen in Fig. 4. In the absence of the SOI, these rules – the spin state is preserved and either n_1 or n_2 is changed by unity – completely determine the allowed two transitions $|0, 0; -\frac{1}{2}\rangle \rightarrow |1, 0; -\frac{1}{2}\rangle$ and $|0, 0; -\frac{1}{2}\rangle \rightarrow |0, 1; -\frac{1}{2}\rangle$. In contrast to the case of circular dots the absorption in the elliptical dot depends strongly on the polarization. This is explained by noting that the oscillator strengths

$$f_{ni} = \frac{2m^* \omega_{ni}}{\hbar} |\langle n | \hat{\mathbf{e}} \cdot \mathbf{x} | i \rangle|^2.$$

actually probe the occupations of quantum states related to oscillations in the direction of the polarization $\hat{\mathbf{e}}$. In a circular dot all oscillation directions are equally probable at all energies implying that the oscillator strengths are independent of the polarization and depend only slightly on the transition energy via ω_{ni} , and the final state quantum numbers $n_{1,2}$. When the dot is squeezed in the y -direction, say, the oscillator states related to the y -motion are pushed up in energy. This means that the polarization being along x -axis most of the oscillator strength comes from transitions to allowed states with lowest energies. Similarly, when the incident radiation is polarized along the y -axis most of the contribution is due to the transitions to the oscillator states pushed up in the energy. In elliptical dots the oscillator states are not pure x - and y -oscillators but their superpositions. Therefore in addition to the main absorption lines, other allowed final states have also non-vanishing oscillator strength. Furthermore, as one can see by looking at the phase space rotation formulas the external magnetic field tends to rotate directions of the oscillator motion causing a shift of the oscillator strength from an allowed transition to another. This is exactly what we see in Fig. 4 (a) and Fig. 4 (d).

Even in the presence of the SOI the two allowed final oscillator states provide major contributions to the corresponding corrected states. Hence we still see two dominant absorption lines. However, now many forbidden transitions have become allowed. The lowest absorption line corresponding to the transition between Zeeman split states with main components $|0, 0; -\frac{1}{2}\rangle$ and $|0, 0; \frac{1}{2}\rangle$ provides a typical example. The transition involves a spin

flip and is therefore strongly forbidden without the SOI. Because the SOI mixes the state $|1, 0; \frac{1}{2}\rangle$ into the former one and the $|0, 1; -\frac{1}{2}\rangle$ into the latter one, the transition becomes possible. The appearance of other new lines can be explained by analogous arguments. There are also additional features involving discontinuities and anti-crossings in Fig. 4. A comparison with the energy spectra indicates that these are the consequences of the anti-crossings present in the energy spectra.

It is also readily verified that the oscillator strengths satisfy the Thomas-Reiche-Kuhn sum rule [17]

$$\sum_n f_{ni} = 1.$$

In terms of the cross section this translates to the condition

$$\int_{-\infty}^{\infty} \sigma_{\text{abs}}(\omega) d\omega = \frac{2\pi^2 \hbar \alpha_f}{m^*}.$$

The absorptions visible in Fig. 4 practically saturate the sum rule, the saturation being, of course complete in the absence of the SOI in panels (a) and (d). The largest fraction (of the order of 1/10) of the cross section either falling outside of the displayed energy scale or having too low intensity to be discernible in our pictures is found at the strongest Rashba coupling in the panels (c) and (f) for large magnetic fields, as expected.

The results presented here clearly indicate that, the anisotropy of a QD alone causes lifting of the degeneracies of the Fock-Darwin levels at $B=0$, as reported earlier [13]. However, for large SO coupling strengths α , the effects of the Rashba SOI, mainly the level repulsions at finite magnetic fields, are magnified rather significantly as one introduces anisotropy in the QD. This is reflected also in the corresponding dipole-allowed optical transitions where the distinct anti-crossing behavior is observed that is a direct manifestation of the anti-crossings in the energy spectra. This prominent effect of the Rashba SOI predicted here could be confirmed experimentally in optical spectroscopy and the Fock-darwin spectra of few-electron QDs [9, 18, 19]. It would also provide a very useful step to control the SO coupling in nanostructures, en route to semiconductor spintronics [3].

The work was supported by the Canada Research Chairs Program of the Government of Canada.

[†] Electronic address: tapash@physics.umanitoba.ca

[2] Y. Oreg, P.W. Brouwer, X. Waintal, and B.I. Halperin, in *Nano-Physics & Bio-Electronics: A New Odyssey*, edited by, T. Chakraborty, F. Peeters, and U. Sivan (Elsevier, Amsterdam, 2002).

[3] For recent comprehensive reviews, see, T. Dietl, D.D. Awschalom, M. Kaminska, and H. Ono, (Eds.) *Spintronics* (Elsevier, Amsterdam, 2008); I. Zutic, J. Fabian, and

- S. Das Sarma, *Rev. Mod. Phys.* **76**, 323 (2004); J. Fabian, A. Matos-Abiague, C. Ertler, P. Stano, and I. Zutic, *Acta Physica Slovaca* **57**, 565 (2007); M.W. Wu, J.H. Jiang, and M.Q. Weng, *Phys. Rep.* **493**, 61 (2010).
- [4] H.-A. Engel, B.I. Halperin, and E.I. Rashba, *Phys. Rev. Lett.* **95**, 166605 (2005).
- [5] Y.A. Bychkov and E.I. Rashba, *J. Phys. C* **17**, 6039 (1984).
- [6] J. Nitta, T. Akazaki, H. Takayanagi, and T. Enoki, *Phys. Rev. Lett.* **78**, 1335 (1997); M. Studer, G. Salis, K. Ensslin, D.C. Driscoll, and A.C. Gossard, *ibid.* **103**, 027201 (2009); D. Grundler, *ibid.* **84**, 6074 (2000).
- [7] H. Sanada, T. Sogawa, H. Gotoh, K. Onomitshu, M. Kohda, J. Nitta, and P.V. Santos, *Phys. Rev. Lett.* **106**, 216602 (2011); S. Takahashi, R.S. Deacon, K. Yoshida, A. Oiwa, K. Shibata, K. Hirakawa, Y. Tokura, and S. Tarucha, *ibid.* **104**, 246801 (2010).
- [8] T. Chakraborty, *Quantum Dots* (North-Holland, Amsterdam, 1999); T. Chakraborty, *Comments Condens. Matter Phys.* **16**, 35 (1992); P.A. Maksym and T. Chakraborty, *Phys. Rev. Lett.* **65**, 108 (1990).
- [9] D. Heitmann (Ed.), *Quantum Materials* (Springer, Heidelberg, 2010).
- [10] J. Königmann, R.J. Haug, D.K. Maude, V. Fal'ko, and B.L. Altshuler, *Phys. Rev. Lett.* **94**, 226404 (2005).
- [11] T. Chakraborty and P. Pietiläinen, *Phys. Rev. Lett.* **95**, 136603 (2005); P. Pietiläinen and T. Chakraborty, *Phys. Rev. B* **73**, 155315 (2006); T. Chakraborty and P. Pietiläinen, *ibid.* **71**, 113305 (2005); A. Manaselyan and T. Chakraborty, *Europhys. Lett.* **88**, 17003 (2009); and the references therein.
- [12] H.-Y. Chen, V. Apalkov, and T. Chakraborty, *Phys. Rev. B* **75**, 193303 (2007).
- [13] A.V. Madhav and T. Chakraborty, *Phys. Rev. B* **49**, 8163 (1994); See also, P.A. Maksym, *Physica B* **249-251**, 233 (1998).
- [14] M.P. Nowak, B. Szafran, F.M. Peeters, B. Partoens, and W.J. Pasek, *Phys. Rev. B* **83**, 245324 (2011).
- [15] A. Singha, V. Pellegrini, S. Kalliakos, B. Karmakar, A. Pinczuk, L.N. Pfeiffer, and K.W. West, *Appl. Phys. Lett.* **94**, 073114 (2009); D.G. Austing, S. Sasaki, S. Tarucha, S.M. Reimann, M. Koskinen, M. Manninen, *Phys. Rev. B* **60**, 11514 (1999).
- [16] W. Zawadzki and P. Pfeffer, *Semicond. Sci. Technol.* **19**, R1 (2004).
- [17] J.J. Sakurai and J. Napolitano, *Modern Quantum Mechanics*, second edition, (Addison-Wesley, New York, 1994), p. 368; W. Thomas, *Naturwissenschaften* **13**, 627 (1925); W. Kuhn, *Z. Phys.* **33**, 408 (1925); F. Reiche and W. Thomas, *Z. Phys.* **34**, 510 (1925).
- [18] L.P. Kouwenhoven, D.G. Austing, and S. Tarucha, *Rep. Prog. Phys.* **64**, 701 (2001); A. Babinski, M. Potemski, S. Raymond, J. Lapointe, and Z.R. Wasilewski, *phys. stat. sol. (c)* **3**, 3748 (2006).
- [19] V. Pellegrini, and A. Pinczuk, *phys. stat. sol. (b)* **243**, 3617 (2006).